ELSEVIER

Chemical Engineering Journal 85 (2002) 273–288

Chemical Engineering Journal

www.elsevier.com/locate/cej

Process development of product recovery and solvent recycling steps of chromatographic separation processes

Jochen Strube [a,*], Robert Gärtner [b,1], Michael Schulte [c]

[a] *Bayer AG, Fluid-Verfahrenstechnik, ZT-TE 5.2/B310, D-51368 Leverkusen, Germany*
[b] *Department of Chemical Engineering, University of Dortmund, D-44221 Dortmund, Germany*
[c] *Merck KGaA, Department SLP Fo BS, D-64271 Darmstadt, Germany*

Received 2 August 1999; received in revised form 18 April 2001; accepted 25 April 2001

Dedicated to Professor Dr.-Ing. Henner Schmidt-Traub, on the occasion of his 60th birthday

Abstract

Chromatography is a separation method which produces product solutions of high purity, but often also with a high product dilution. In this study, feasible strategies for downstream processing of typical chromatographic product solutions were developed theoretically. The unit operations membrane processes, precipitation, crystallization, and evaporation, proved to be the most suitable for the treatment of chromatographic product solutions. Computer models of these unit operations were made to simulate the chosen refining strategies. The results of the process simulation for the drug intermediate product EMD 53986 (5-(1,2,3,4-tetrahydroquinoline-6-yl)-6-methyl-3,6-dihydro-1,3,4-thiadiazine-2-one) are given to exemplify the quality of the data process simulation can supply for process planning and for equipment design. An overview is given. The specific demands of small drug molecules are pointed out by describing the contrary proceedings of the other groups of molecular compounds like small and larger biologically active compounds.

For many chromatographic separations, different continuous and discontinuous chromatography methods are available. In this study, the efficiency of common batchwise chromatography and continuous simulated-moving-bed (SMB) chromatography were compared by the, respectively, required refining steps for isolating the product from the chromatographic product solution.

Keywords: Process simulation; Downstream processing; Chromatography; Simulated-moving-bed; Enantiomers

1. Introduction

1.1. Product recovery and solvent recycling

Chromatography is a process of selective adsorption of the target molecules from a solvent onto an adsorbent. By flushing the adsorbent with a desorbent solvent, the compounds of a mixture are driven at different speeds through the chromatographic bed and can be collected separately in pure form at the end of the bed. In chromatographic separations, very high product yields and purities of 99% and more can be achieved.

The main goal of the subsequent refining processes is to maintain the product specification achieved in the chromatographic separation and to yield the product in a more concentrated form. The valuable main product after a chromatographic separation step is therefore present in high purity, but it is in most cases highly diluted in the process solvent. This makes it necessary for its further processing or final formulation to isolate it as efficiently as possible from the product solution. Additional refining steps for conserving, confectioning, and conditioning are not only dictated by the physical properties of the product substance, but also by the products later use.

The development of refinement strategies for such product solutions is a classical subject in process design, and for the handling of such problems process simulation has proved to be a suitable tool. For preliminary evaluation of different process alternatives for example quantitative data is necessary. To be able to correlate physical effects and dependencies of process parameters, physical and chemical models are needed.

In a first preliminary study [1], models for a choice of unit operations were gathered and implemented into the process simulation package SPEEDUP^{TM} (AspenTech Inc., MA, USA) for the development of refining strategies after

* Corresponding author. Tel.: +49-214-30-67278; +49-214-30-81554.
E-mail address: jochen.strube.js@bayer-ag.de (J. Strube).
[1] Present address: Laboratory for Process Equipment, Delft Technical University, 2628 CA Delft, The Netherlands

1385-8947/02/$ – see front matter
PII: S1385-8947(01)00171-1

Nomenclature

Variables of Section 3.1: reverse osmosis and ultrafiltration models

A_M	membrane surface area (m^2)
A^*	osmotic permeability for solvent (s/m)
B^*	osmotic permeability for product (s/m)
D_{iw}	diffusion coefficient (m^2/s)
k	mass transfer coefficient (m/s)
k_1	Langmuir coefficient
$\dot{m}$	mass flow (g/s)
$\dot{m}''$	area-specific mass flow/mass flow density (g/m^2 s)
p_M	pressure in the membrane (Pa)
Δp	operating pressure (Pa)
R	retention rate
R_M	permeation resistance factor of the membrane (l/m)
t	time (s)
w	mass fraction of a component (wt.%)
w_{iMF}	mass fraction of i at the feed-side membrane surface (wt.%)
w_{iMP}	mass fraction of i at the permeate-side membrane surface (wt.%)
y	vertical coordinate (m)
z	horizontal coordinate (parallel to membrane surface) (m)

Greek letters

δ	diffusion border layer (m)
η	dynamic viscosity (Pa s)
ν_P	area-specific permeate flow (m^3/m^2 s)
$\Delta\pi$	osmotic pressure (Pa)
ρ	solution density (g/ml)

Indices of Section 3.1

F	feed/feed-side
i	component i (product)
M	membrane
P	permeate/permeate-side
w	component w (solvent)
y	vertical coordinate

Variables of Section 3.2: evaporation model (rotating film evaporator)

A_H	heater surface area (m^2)
c_{PF}	specific heat capacity of the feed (kJ/kg K)
Δh_V	specific heat of evaporation (kJ/kg)
k	heat transmission coefficient (kW/m^2 K)
$\dot{m}$	mass flow (kg/s)
$\dot{m}''$	area-specific mass flow/mass flow density (kg/s m^2)
M_w	molar weight of the solvent (g/mol)
q_H	heating power density (kW/m^2)
Q_H	heater power (kW)
r_a	outer radius of the heater tube (m)
r_b	inner radius of the heater tube (m)
R	ideal gas constant = 8.3144 (J/mol K)
T_{bp}	boiling point (K)
T_F	local feed solution temperature (K)
T_H	temperature of the heating utility (K)
ΔT_{bp} (dw_{iF})	increase in boiling point by rising product concentration (K)
w	mass fraction (wt.%)
x_i	mole fraction of the solute (product) (mol%)
z	coordinate along the heater surface (m)

Greek letters

α_a	heat transfer coefficient on the outside of the heater tube (heating medium) (kW/m^2 K)
α_b	heat transfer coefficient on the inside of the heater tube (product side) (kW/m^2 K)
λ_W	thermal conductivity of the tube wall (kW/m K)

Indices of Section 3.2

a	heater surface in contact with the heating medium/utility (outside of the tube)
b	heater surface in contact with the product solution (inside of the tube)
D	evaporated solvent/steam
F	feed (product solution)
H	heater
i	solved product
w	solvent

Variables of Section 3.3: mixed-solution-mixed-product-removal (MSMPR) crystallization model

A	total crystallite surface (m^2)
B	nucleation rate (l/s m^3)
c	concentration (g/l)
c_D	concentration at the crystal surface (kg/m^3)
c^*	saturation concentration (g/l)
C_1, C_2	empirical constants of the component system
$\dot{D}_K$	removed solvent stream (e.g. by evaporation) (g/s)
f_A	surface form factor (relative to perfect sphere)
G	radial crystal growth rate (m/s)
k_d	mass transfer coefficient (m/s)
k_R	reaction rate coefficient (m/s)
L	crystal diameter (m)
$\dot{L}$	feed to crystallizer (g/s)
$\dot{m}$	rate of crystallization (kg/s)
n	reaction order
n_i	number of crystals of diameter class i per volume (l/m^4)
n_{i0}	nucleate density (l/m^3)
$\dot{S}$	produced crystallite mass flow (g/s)

V	crystallization volume (m^3)
$\dot{V}$	volume flow of feed through the crystallizer (m^3/s)
w_1	mass fraction of crystallizing compound in the feed (wt.%)
w_2	mass fraction of remaining solved crystallizing compound (wt.%)

Greek letters

μ	dry weight fraction of the recovered wet crystals (g dry substance/g crystallite product)
τ	mean residence time (s)

Variables of Section 3.3: protein precipitation model

c_P	concentration of the growing particles (nuclei); start concentration of the protein (mol/m^3)
d_P	particle diameter (m)
D_{iw}	diffusion coefficient of component i (salt or protein) (m^2/s)
D_{Pw}	diffusion coefficient of the growing particles (m^2/s)
l	mean diameter of mixing eddies (m)
N_A	Avogadro's number $= 6.023 \times 10^{23}$ (l/mol)
P	mixing power of the stirrer (W)
$\sqrt{P/V(\rho\nu)}$	mean velocity gradient of the mixing (l/s)
t	time (s)
t_M	required mixing time (s)
V	reactor volume (m^3)

Greek letters

α	fraction of particle collisions with resulting aggregation
κ	protein agglomeration rate constant (perikinetic growth) ($m^3/mol\,s$)
ν	kinematic viscosity of the solution (m^2/s)
ρ	density of the solution (kg/m^3)

chromatographic separations. This also allowed an effective evaluation of the process alternatives. The models were constructed in a generally applicable form for different groups of product substances to allow a great degree of flexibility in their use.

The unit operations are as follows:

I. Precipitation processes
   1. Crystallization
   2. Protein precipitation

II. Membrane processes
   3. Ultrafiltration
   4. Reverse osmosis

III. Evaporation
   5. Rotating film evaporator

The unit operations were chosen considering the general product properties, separation efficiency, separation quality, and process economy. In case of especially valuable products, e.g. drug intermediates or final pharmaceutical products, possible reductions in plant cost are second in priority to minimizing the product loss in the refining process.

Typical chromatographic separation systems can be grouped into the following categories.

1. Proteins separated by reverse-phase chromatography: As a final polishing step in small protein separation, reversed-phase (RP) chromatography is a widespread technique. The molecular weight of these proteins is $\geq$3000 g/mol. An aqueous solvent is used, as the material of the chromatographic column is hydrophobic (=reversed phase). The solvent is usually composed of water mixed with organic additives (methanol, acetonitrile, often ethanol, isopropanol, etc.) to modify the retention of the product component. Often a buffer has also to be added, as the solubility of proteins is highly dependent on the pH. A typical example for this class of separations is the final purification of insulin. Separation of these types of components is extensively reviewed in [2] and is not within the scope of this work.
2. Smaller proteins and peptides separated by normal-phase chromatography: The molecular weight of these peptides is about 1000 g/mol. The employed solvents are generally composed of alkanes and/or alcohols like hexanol and heptane, and also, e.g. dioxane and ethyl-methyl-ketone. Separations take place on reversed-phase or normal-phase silica. Classical examples are the purification of cyclosporin, vancomycin, or taxol.
3. Complex organic compounds/molecules such as, e.g. synthetic enantiomers and monosaccharides: These compounds are separated by normal-phase or chiral chromatography. They have a molecular weight of about 200 g/mol. For the chromatography, they are solved in alkanic and alcoholic solvent systems like methyl-cyclohexane, ethylacetate, or ethanol.

To exemplify the application of process simulation, a refining strategy for the product EN 21 (a racemic mixture, also categorized as EMD 53986) is developed and its parameters are calculated. EMD 53986 is 5-(1,2,3,4-tetrahydroquinoline-6-yl)-6-methyl-3,6-dihydro-1,3,4-thiadiazine-2-one (Fig. 1) and has a molecular weight of about 261 g/mol. It is a typical class 3 compound. It is solved in a mixture of 5% ethylacetate and 95% ethanol [3].

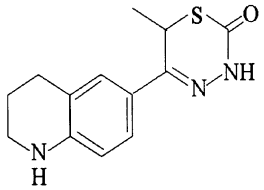

Fig. 1. Molecular structure of EMD 53986 (EN 21).

The separation conditions for this drug intermediate were thoroughly examined [3,4]. In a first study, a comparison between classical batch chromatography and continuous counter-current chromatography (simulated-moving-bed (SMB) chromatography) was undertaken, especially with regard to the economic parameters of the separation (Strube OPRD, 1998). For details of the principle of SMB chromatography, see [5]. The property data of this compound was either supplied by Schulte [6] or estimated based on the molecular structure with ASPEN PLUS^{TM}. Estimates were checked for reliability by comparison with data of aromatic substances with similar molecular weights [7]. The properties of the solvent mixtures were also estimated with ASPEN PLUS^{TM} for operation conditions (temperature, pressure, and concentration). They were again verified by interpolating the property values of the pure components [7–9].

1.2. Process development—combining the necessary unit operations

The choice of the employed unit operations is determined by some simple technical considerations. As the product should be isolated as a pure substance after chromatographic separation, it has to be either precipitated from its solution or the solvent has to be evaporated to acquire the pure solid. To cause its precipitation, the product has to be concentrated first beyond its saturation point in the solution. This can be achieved either by membrane processes or again by evaporation. For process economy, the recycling of the removed solvent for reuse in the chromatographic separation should be considered. Following this strategy, the following generalized process outline can be sketched (see Fig. 2).

In the first step, the product solution of the chromatographic separation is concentrated by a membrane process to saturation. The saturation concentration depends on the product and the solvent, and is difficult to implement empirically. In a membrane process, the product should not be concentrated beyond the point of saturation or fluidity, because this could result in damaging or clogging the membrane. As membrane processes need considerably less energy than evaporation, they are usually more efficient at low concentration ranges.

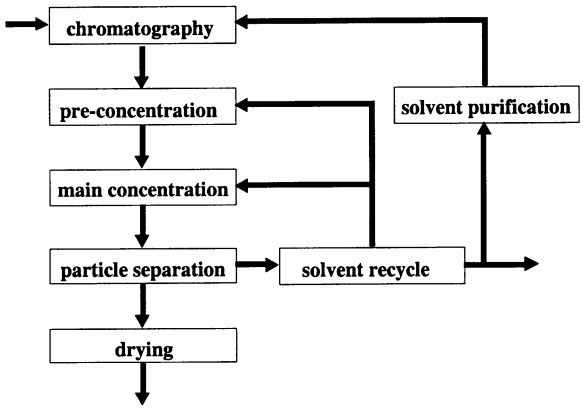

Fig. 2. Flowsheet of the product recovery and solvent recycling operations.

After reaching saturation, the product solution gets into the main concentration step. Here the product is separated from the remaining solvent by evaporation or precipitation, e.g. crystallization. If precipitation results in particle suspension, these particles have to be recovered from the remaining sated product solution by a particle separation step. This can be done by sedimentation, microfiltration, or a hydrocyclone, depending on the component system. Important parameters are the density difference of product and solution, the suspension viscosity and the particle size distribution.

The recovered solid is then stripped of adhering solvent in a final drying step. If the product cannot be precipitated, the solution has to be concentrated to the limit of fluidity and then stripped of the remaining solvent in a dryer to produce the pure solid.

The removed solvent can be split into its components to be reused in the chromatographic separation. The purification of the solvent of product traces can prove difficult, but can be worthwhile, considering the reduction in the amount of required solvent [10]. But as impurities, e.g. caused from remaining product traces, can accumulate in the recycle, it seems better to dispose off used solvent fractions with low product concentrations than risk contamination in the chromatographic system by recycling the used solvent. The removal of these impurities or product traces is also vital for the chromatography, as they can poison the chromatography column. They would reduce the desorbing power of the eluent solution, with which they would be given into the column.

On the other hand, it can prove necessary for process efficiency to recycle solvent fractions with high remaining concentrations of product to the first or the main concentration step. Those steps have to be scaled up for the higher input of feed combined with recycle. It has to be considered that recycling can even produce impurities from solvent and/or product components due to the higher mean residence time of the solution in the process caused by the recycle.

In pharmaceutical production at any form of recycle of material, it has to be proven by quality assurance and control methods that cross-contamination is avoided. The proper specification of the recycle has to be assured.

The efforts of quality assurance and control have to be evaluated against the benefits of recycling which is intended to decrease product losses and/or save solvent/buffer/detergent amounts.

1.3. Choice of refining strategy

Summarizing the arguments outlined in Section 1.2, two possible refining methods can be identified.

Peptides and proteins, which cannot be crystallized, can be isolated after chromatographic separation steps and proceeding ultrafiltration/diafiltration steps by protein

precipitation or vacuum evaporation ending with a freeze drying/lyophilization. But, components of lower molecular weight, as the described enantiomer, amino acids, oligopeptides or saccharides, can be recovered by

- evaporation,
- crystallization.

The final decision on the refining strategy depends on the physical properties of the component system of the solution. Foremost, it depends on the stability of the compounds at rising temperatures and sharp increases in temperature, but also on the crystallizability of the product compound, its solubility in the solvent, the solvent's specific heat of vaporization and the solution viscosity at high product concentrations.

By some simple prior technical deliberations, this decision can be greatly simplified. Because the gathering of property data usually requires a great deal of time and engineering know-how, the amount of required data should be kept reasonably small by a first choice on the processes and unit operations to be modeled. Therefore, the general advantages and disadvantages of the process alternatives should be weighed against each other before beginning with the modeling.

The solubility of biomolecules is quite low and products are extremely diluted. Therefore, chromatographic separations of proteins and peptides are operated at low product concentrations, but near to the solubility margin. A first concentration step like a membrane process might not be needed for the recovery of proteins. And as the physical limit of membrane processes is usually product saturation, as precipitating product can spoil membrane permeability, the membrane process is not the tool of choice here. Hence the process can be simplified to the steps precipitation, particle recovery, and freeze drying (lyophilization) as one possibility or vacuum evaporation and freeze drying as the other.

The main advantage of vacuum evaporation compared to protein precipitation techniques lies in the fact that the remaining solution after precipitation still contains a high amount of product. This product fraction has either to be recovered in additional process steps or is lost with the waste solution. Furthermore, the vacuum evaporation can be operated continuously and includes fewer process steps than the precipitation. Thus, the evaporation process appears less prone to failures.

Also there is no need for additives as used to induce precipitation, which would later remain in the product or would have to be extracted by additional purification steps.

The main disadvantage of vacuum evaporation is the complicated and expensive equipment needed to maintain short evaporator residence times and the vacuum. An additional disadvantage is the amount of energy needed for vaporization and maintenance of the vacuum. Especially with proteins, the vacuum is needed to reduce the boiling point of the solution, as proteins are usually very sensitive to temperatures above 40 °C. To maintain this low temperature in the evaporator, a medium of heat transfer with high energy content at low temperature level is needed, e.g. subatmospheric steam. Finally, the direct concentration by evaporation is still too strenuous for many higher proteins due to the hardly controllable solvent removal from the protein. Therefore, a sequence of different chromatography unit operations is applied in combination with ultrafiltration at the beginning to clear of particles and diafiltration at the end to get rid of salts. After fermentation, there is a capture step. Usually, ion exchangers are suitable. Afterwards, most common is a chromatography sequence of ion exchange (anion and/or cation) combined with affinity chromatography for the main purification steps. For the final polishing steps generally ion exchange, reversed phase, and size exclusion are used. All contaminants and impurities like, e.g. host cell proteins, total proteins and fragments, DNA, solvent/detergents as well as metal ions and salts are cleared specifically over a wide range of 2–6 logs at each step. The product is concentrated by that about a factor of 10–100.

In contrast to that, the refining strategy for small molecules which can be well/better characterized by analytical methods is simpler. Substances that can be recovered by crystallization, like enantiomers and short-chained peptides, should just be supersaturated in the solution and not be fully dried by evaporation as crystallization produces a more stable product, which in addition is easier to handle. The individual final formulation steps of each product in order to apply the drug efficient to the patients dominates the stability and reliability of a drug manufacturing process extremely.

To reduce energy costs, the solution can be concentrated close to saturation by a membrane process instead of evaporation. This is especially feasible, if saturated or even supersaturated solution from the crystallization is recycled into the evaporator, as the risk of scaling in the evaporator and the involved piping increases with increasing product concentration. The heater area and also the mean residence of the evaporator can be reduced, if the feed solution is pre-concentrated in a previous membrane step. To counter scaling by crystallization in the evaporator, a special type of heat exchanger with scrapers (to remove scaling) and low residence times (to undercut the induction time of crystallization) has to be employed, which increases the equipment cost drastically. A reduction in size and thus heater area is recommended here. This reduction can also be achieved by prior concentration with a membrane process.

The recycling of the remaining solution after crystallization is strictly recommended, as this solution is still supersaturated with product. This solved fraction can amount to 50% and more of the total product, as simulations with a mixed-solution-mixed-product-removal (MSMPR) model indicate.

The alternative method to recycling would be to add additional supersaturation and crystallization stages. As the feed stream would diminish from stage to stage, controlling the concentration and crystallization steps would become more and more difficult. Also the equipment cost for such

a multistage process is definitely higher than for the recycling method, which only requires a scale-up of the main equipment.

When using a recycling strategy, the recycle stream and the size of the evaporator have to be dimensioned for a shorter residence time in the evaporator than the induction time of the crystallization. Undercutting induction time is only feasible as far as all crystallites in the recycle are redissolved at the evaporation temperature. Otherwise seeding could induce premature crystallization and thus scaling in the evaporator. To avoid this, the introduction of scrapers to remove scaling from the heater surfaces would be a possible countermeasure.

An additional advantage of crystallization is the reduction in vaporization energy, because the crystals can be easily recovered by a particle separator without vaporizing the remaining solvent. Vaporization would get even more difficult, as heat and mass transfer conditions become more unfavorable with increasing product concentration.

2. Process modeling

The proposed refining strategies have the following principal structures.

- In the first step, the solution from the chromatographic separation is pre-concentrated to a limit defined by process conditions or the capability of the applied unit operation.
- In the second step, the product component is isolated from the process solution.
- After that, a major product fraction can be recovered in a particle/solid separator as the third step.
- The remaining solution is then recycled to one of the concentration steps or disposed off as waste depending on its product content.

  In solvent recycling steps, the solvent mixture is split into its components for reuse in chromatography. This can be done by, e.g. distillation or pervaporation. If the solvent recycling is likely to spoil the purity of the product, the remaining process solution should not be recycled, but directly be disposed off as waste.
- The product refining can be concluded with a final drying or solvent-stripping step.

Depending on product requirements and the product condition, additional refining steps can become necessary (e.g. re-crystallization, washing, stripping, adding of conservation agents). As this would become too specific for this study, it will not be discussed further.

The aim of this work is the simulation of the main steps of the product recovery after chromatographic separations as outlined above. The simulation employs current mathematical models of the applied unit operations. For theoretical background on the modeled process steps see Chapter 3 which reviews the literature on the relevant unit operations. The unit operation models of solvent recovery and product concentration steps are explained in this paper specifically. Only the chromatographic models have already been described in detail before [11].

2.1. Validation of the computer models

On the basis of the mathematical modeling, computer models of the unit operations were created using the flowsheet simulation package SPEEDUP^{TM}. These were used to simulate the described refining process alternatives.

The validity of these models was checked in an extensive series of calculations with parameter variation, simulation studies, and comparison with literature.

The programs were analyzed for programming and modeling errors and corrected, if simulation results produced unrealistic results. This should ensure the reliability of the models in their specific operation ranges.

In detail, the computer models were checked by the following procedures.

1. The mass and component balances for each unit operation were automatically calculated in each simulation. Although, unity in the balances does not prove the models to be free of modeling or programming errors, it does prove that all inputs and outputs were correlated and taken into account in the model.
2. To detect and eliminate modeling and programming errors, parameter studies were performed. By comparison of the simulation results with data from literature, the model behavior under variation of plant and process parameters and the accuracy of the simulation results were verified. Borderline conditions and parameter developments were studied.
3. The numerical deviations of the model calculations were checked by varying the convergence tolerance of SPEEDUP^{TM} in the parameter studies. All models converged up to a relative accuracy of 10^{-5} to produce a feasible solution. As the membrane and evaporation models had to be calculated stepwise along the length of membrane or evaporation area, the step-length was also varied to analyze its influence on the simulation accuracy.
4. Finally, in the performed process optimization, the model sensitivity on the optimized parameters was examined. As specific component data was used in this step, the results were specifically compared to experimental data and process results in literature.

2.2. Process optimization by computer simulation

The aims of process optimization can be summarized with varying priorities as follows:

- reducing production costs by minimizing plant and utility costs for a specified production capacity or optimizing the production capacity of a given plant;
- enhancing product purity and/or yield;

- enhancing the reliability of a production plant, i.e. the reliability of the process;
- improving pollution control, i.e. adaptation to pollutant limits and other restrictions.

One aim of this study was to quantify the equipment required of the process alternatives and to dimension this equipment favorably.

The main goal in the case of EN 21 was maximizing product purity and yield. The next important priority was assigned to equipment cost for selecting the most economically favorable process alternative.

This method of process selection was not only employed to evaluate the refining processes, but also to compare batch and SMB chromatography as the source of the solutions to be processed. As the composition of the chromatographic product solution can influence the efficiency of the recovery in the downstream processing stages, the chromatography method can influence the expense required in the downstream processing. The comparison of the required refining steps can therefore yield a valuable argument for the selection of a chromatographic technique.

3. Example: refinement of EMD 53986 (EN 21)

The process selection for the refinement of EMD 53986, a typical compound of low molecular weight, is simplified by the fact that this product can be crystallized. The alternative refining procedures for products that cannot be crystallized are discussed in Section 2. As isolating the product completely by evaporation can result in considerable encrusting in the evaporator, which again could result in impairing product quality, evaporation cannot be recommended as the main concentration step.

The selected unit operations are rather as follows:

1. *reverse osmosis* as primary concentration step;
2. *evaporation* to achieve supersaturation;
3. *crystallization* employing the MSMPR method;
4. *particle recovery*;
5. *recycling* of the remaining solution from the particle separator back into the evaporator;
6. drying or stripping to remove adhering solvent rests.

Of the listed process steps, only the italic ones were computer modeled, calculated, and preliminarily optimized based on the simulation results.

The processed feed streams are given here. They were determined and optimized in a previous study [11]. As process optimization is mainly of interest for industrial-scale production, the experimental results of the laboratory-scale chromatographic equipment were extrapolated for a corresponding industrial production amount. The process streams were thus calculated for an equivalent column diameter of 40 cm (16 in.) for the SMB chromatography. The batch chromatography was scaled up accordingly. The scale-up factor between the laboratory-scale equipment and the production equipment is 236-fold (Fig. 3).

The mass of the refined pure, dry product would amount to about 3 tonnes per year from 500 to 3000 tonnes per year of product solution from the chromatographic separation assuming an operation time of 24 h per day and 330 days per year. This is a realistic figure for a drug substance to be purified by chromatography.

The batch chromatography is discontinuous. To be able to draw a comparison between the continuous SMB chromatography process and the batch process, and because the refining process is also by design continuous, the raffinate and extract amounts per run were translated into equivalent raffinate and extract streams. These equivalent streams were

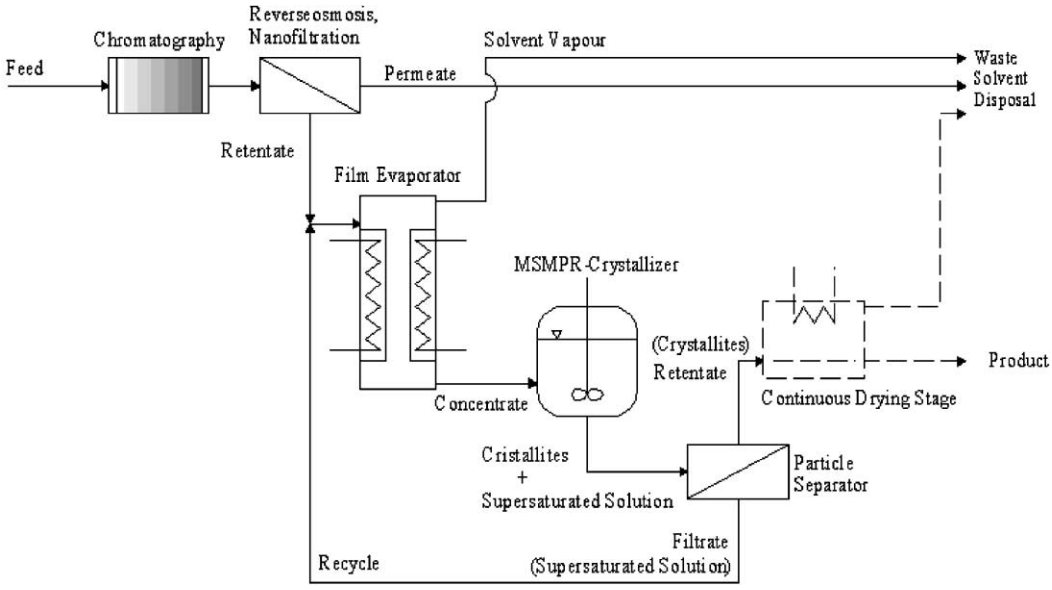

Fig. 3. Flowsheet of the crystallization of EMD 53986 (EN 21).

calculated by dividing the rfespective amounts per chromatographic separation run by the cycle time. The cycle time of one separation run consists actually of the injection time and the sum of the subsequent elution times of the different product components.

The process was simulated for both batch and SMB chromatography for both of the two calculated feed streams, the raffinate and the extract stream of the respective chromatography methods. The feed streams are called extract and raffinate following the nomenclature for SMB separations.

The extract and raffinate streams were determined to be as follows:

extract:

- from batch chromatography: 118.99 g/s containing 0.93 mg product/g solution;
- from SMB chromatography: 76.85 g/s containing 1.32 mg product/g solution;

raffinate:

- from batch chromatography: 25.761 g/s containing 4.3 mg product/g solution;
- from SMB chromatography: 14.943 g/s containing 6.87 mg product/g solution.

The desired enantiomer of EMD 53986 (EN 21) is actually only contained in the extract, as the raffinate contains the structural counterpart which is produced in the synthesis in the same amount as the main product. It has no actual use and is a waste product in this process. As the difference in the order of magnitude of the extract and raffinate streams allows us to demonstrate the influence of the size of the product stream on the refining process, the treatment of both streams was simulated without further regard on the usefulness of the respective product.

The enantiomer is >99% pure in raffinate and extract after chromatographic separation, therefore no product selectivity considerations for the single unit operations have to be taken into account. The solvent is a mixture of ethylacetate and ethanol (95/5 vol.%).

From these outlining parameters, the computer simulation and the optimization based upon it resulted in the following process parameters for the unit operations.

3.1. (A) Reverse osmosis versus ultrafiltration

The product solution from the chromatographic separation can be concentrated by reverse osmosis to the point of saturation. The saturation concentration of the compound EN 21 in the used solvent is about 13.0 g/l referring to information from Merck KGaA [6]. This amounts to a weight fraction of about 14.4 mg/g. As both streams, raffinate and extract, contain the same quantity of product (but different amount of solvent), they can all be reduced to 7.5 g/s containing in average 14.4 mg product/g solution. This is only valid if the mixture to be separated is a 1:1 mixture of two-product compounds and if complete separation of the two products is achieved, as it is in this case. Otherwise, total and component mass balances have to be made to calculate the product amounts.

By using reverse osmosis instead of evaporation, a great amount of energy can be saved. To concentrate the batch-extract-stream of 118.99 g/s to the saturation concentration of the product, about 111.5 g/s of solvent has to be removed. Using reverse osmosis with 20 bar operating pressure, this would require about 265 W to maintain the operating pressure plus the power for pumping the solution through the modules (to overcome pipe friction in the modules).

Evaporating 111.5 g/s of solvent requires on the other hand (without considering the energy for heating to boiling conditions and the increase in the boiling point due to the solved components) about 47.5 kW.

3.1.1. Models

The computer-based simulation of reverse osmosis processes has already been discussed in several publications, e.g. [12–15]. Niemi and Palosaari [13,14] and Mehdizadeh and Dickson [15] employ phenomenological models, which only enable reliable predictions of permeate flux and product loss after acquiring extensive experimental data on the process system or require an unhandy amount of mathematical computing.

As the physical background of the model described by Rautenbach [12] offers an easy comprehensible method for predicting membrane permeability for different compounds, such as the product and the solvent in our application, it was used for the modeling of the reverse osmosis module.

3.1.1.1. Ultrafiltration model. Assumptions of the ultrafiltration model by Rautenbach [12] (Fig. 4) are as follows:

1. stationary conditions at the membrane (i.e. $\partial w_i/\partial t = 0$);
2. negligible concentration gradients parallel to the membrane surfaces;
3. no chemical reactions in the medium (no component loss or increase);
4. the convective mass flow from the bulk onto the membrane surface is equal to the permeate flow (simplified mass balance: $\dot{m}_y = \dot{m}_\mathrm{P}$);
5. High and constant local retention rate R of the membrane ($w_\mathrm{P} = (1 - R)w_\mathrm{F}$).

- Concentration boundary layer at the membrane surface on the feed-side:

$$\frac{w_{i1} - w_{i\mathrm{P}}}{w_{i2} - w_{i\mathrm{P}}} = \exp\left(-\dot{m}''_\mathrm{P}\int_0^\delta \frac{\mathrm{d}y}{\rho D_{iw}}\right) = \exp\left(-\frac{\dot{m}''_\mathrm{P}}{\rho k}\right),$$

  $k = D_{iw}/\delta$ is the mass transfer coefficient.
- Permeate flow density:

$$v_\mathrm{P} = \frac{\Delta p - \Delta\pi}{\eta_\mathrm{P} R_\mathrm{M}} = \frac{\dot{m}''_\mathrm{P}}{\rho_\mathrm{P}}.$$

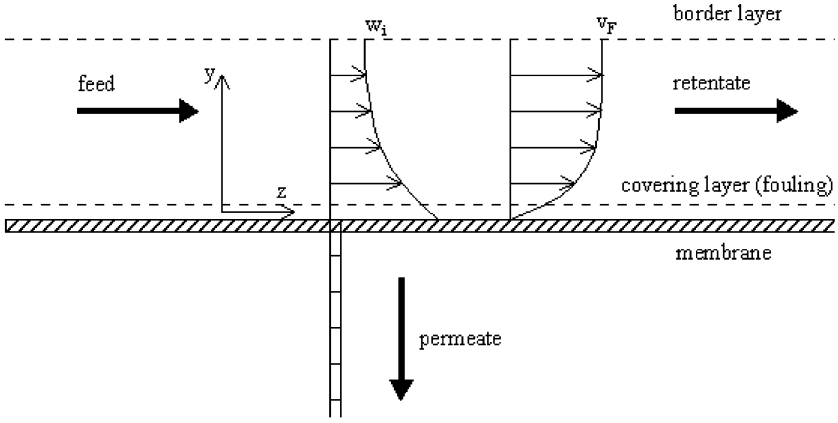

Fig. 4. Border layers of the ultrafiltration model.

- Mass balance equations are as follows:
  - Mass balance (at a surface increment dA_M):

    $$d\dot{m}_F(z) = -d\dot{m}_P(z) = -\dot{m}''_P(z)\,dA_M.$$

  - Component balance:

    $$\dot{m}_F(z)\,dw_F(z) + d\dot{m}_F(z)w_F(z) = -\dot{m}''_P(z)w_P(z)\,dA_M.$$

- Grade of product loss:

  $$w_P = (1 - R)w_F.$$

3.1.1.2. Reverse osmosis model. Assumptions of the model by Rautenbach [12] (Fig. 5) are as follows:

1. the membrane is regarded as a continuum (similar to a phase);
2. there is equilibrium between membrane surface and feed or permeate, respectively, for each of the solution components;
3. couplings of the partial flows of the permeating components can be neglected;
4. constant pressure in the membrane; no pressure gradient in the membrane ($\partial p_M/\partial y = 0$);
5. the concentration of a component i in the membrane can be calculated by a sorption isotherm (for example a Langmuir isotherm: $w_{iM} = k_1 w_{iF}/(1 + k_1 w_{iF})$).

- Partial permeate flow densities for the binary system solvent w and solute i:

  $$\dot{m}''_w = A^* \frac{1}{1 + k_1 w_{iF}}(\Delta p - \Delta\pi_w),$$

  $$\dot{m}''_i = B^* \frac{k_1 w_{iF}}{1 + k_1 w_{iF}}(\Delta p - \Delta\pi_i).$$

- Feed-side concentration boundary layer:

  $$\frac{w_{i1} - w_{iMF}}{w_{i2} - w_{iMF}} = \exp\left(-\dot{m}''_P \int_0^{\delta_F} \frac{dy}{\rho D_{iw}}\right) = \exp\left(-\frac{\dot{m}''_P}{\rho k_F}\right).$$

- Permeate-side concentration boundary layer:

  $$\frac{w_{i3} - w_{iMP}}{w_{i4} - w_{iMP}} = \exp\left(-\dot{m}''_P \int_0^{\delta_P} \frac{dy}{\rho D_{iw}}\right) = \exp\left(-\frac{\dot{m}''_P}{\rho k_P}\right).$$

- Mass balance analog to ultrafiltration.

The simulation with this model produced for the present component system, an area- and pressure-specific permeate

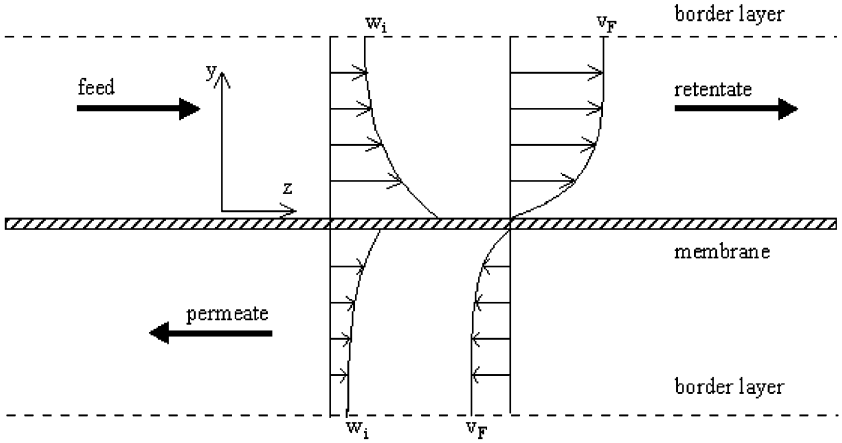

Fig. 5. Border layers of the reverse osmosis model.

flux (permeability) of about 1.5 g/MPa s m^2. This value is in good correlation with the results of Niemi and Palosaari for the similar solvent systems acetic acid and ethanol, which where calculated to be about 1.56 g/MPa s m^2 for acetic acid and about 1.66 g/MPa s m^2 for ethanol.

Also the range of permeabilities for reverse osmosis of aromatic compounds in an ethanolic solvent employing commercial membranes listed by Knauf [16] coincide well with our relatively simple estimation. The range of the cited permeabilities stretches from 0.5 g/MPa s m^2 for the system ethanol–xylol to 1.75 g/MPa s m^2 for the system ethanol–cyclohexane.

The most difficult step in purely theoretical modeling of reverse osmosis is estimating the retention rate for the solved product. Referring to Petersen, the retention rate for non-ionic substances of a molecular weight of about 200 g/mol, like our product (261 g/mol) is already about 80–99% with unspecific commercial membranes as employed in the desalination of seawater [17]. Therefore, the model is adjusted to imply a retention rate of more than 98% to reflect the use of a sophisticated organic separation membrane.

The retention rate in reverse osmosis cannot be set as a fixed parameter like in ultrafiltration. It depends strongly on the concentration profile in the module and can change significantly with varying input parameters, e.g. starting concentration. It can be generally remarked though that the product loss increases and thus the retention rate decreases with increasing operating pressure. Whether this increase is significant is highly dependent on the membrane and the component system.

The reverse osmosis step acts as a pre-concentrating stage to achieve product saturation in the solution. Therefore, it is independent from the following process steps and can be analyzed and optimized independently from the rest of the process. For the optimization of the reverse osmosis modules, the following parameters are the most relevant ones.

- The required membrane surface area, as it determines the cost of the membrane module.
- The applied operating pressure, as it determines the area-specific permeate flux (membrane area-specific volume flow (m^3/m^2 s)). Increasing pressure increases the permeate flux and enables a reduction in membrane area and thus module cost, but it also increases the energy cost for generating the pressure difference and to some extent product loss.
- The product transmission is equal to product loss in reverse osmosis. It increases with operating pressure, as the product permeates the membrane by the same mechanism as the solvent. Also a possible reuse of solvent would get more difficult with increasing product content in the recycled solvent.

As the product is a valuable pharmaceutical compound, its loss and thus the product transmission should be minimized. This implies that the equipment cost should not be lowered by reducing membrane area by increasing the operating pressure. The lower limit for operating pressure in reverse osmosis according to Rautenbach is 20 bar [12,18]. An increase of the pressure by 50% (from 20 to 30 bar) would also result in an increase in permeate flux of approximately 50%. With this, the effective membrane area could be reduced by one-third. As this would also decrease product retention, the product transmission would increase by 10%. As this cannot be accepted, the lower pressure regime of 20 bar is applied.

Increasing the feed flow velocity in the module can reduce the product loss, as this diminishes concentration polarization at the membrane surface. This can be achieved without changing the process streams by reducing the effective width of the membrane surface. As this modification also results in increasing the membrane length by the same factor, this is only efficient for the treatment of the smaller raffinate streams. Here the width of the module is decreased to 50% to double flow velocity in the module.

As pressure loss by friction is not heeded in the model, but does increases proportionally with membrane length, its influence on the driving transmembrane pressure (=operating pressure) can no longer be neglected with further reducing membrane width and increasing membrane length. Otherwise, this would result in substantial errors in calculating permeate flux and thus in the module model.

But also a minimal flow velocity of 5–10 cm/s should be maintained in the module. The maximal membrane width for a minimum flow velocity of 5–10 cm/s is 20 cm for the extract streams, which leads to membrane lengths of more than 100 m. Similar ratios were also employed in dimensioning the membrane area for the treatment of the raffinate streams.

The model equations for reverse osmosis are listed in Chapter 3. The essential results of the dimensioning of the reverse osmosis stage by the simulation are given in Table 1.

As can be seen from Table 1, increased dilution of the feed stream has a negative impact on the refining efficiency.

Table 1
Results for dimensioning the reverse osmosis module

Reverse osmosis	Batch chromatography		SMB chromatography	
	Extract	Raffinate	Extract	Raffinate
Feed				
Rate (g/s)	118.99	25.761	76.85	14.943
Amount (mg/g)	0.93	4.3	1.32	6.87
Concentrate				
Rate (g/s)	7.62	7.63	7.07	7.154
Amount (mg/g)	14.3	14.5	14.1	14.3
Membrane				
Area (m^2)	38.2	6.4	24.2	2.8
Width (m)	0.2	0.05	0.2	0.025
Pressure (bar)	20	20	20	20
Product loss (mg/s)	1.863	0.673	1.617	0.337

For higher dilution rates, a larger membrane area is needed to concentrate the solution to the saturation concentration of 14.4 mg/g. Also the product loss increases almost proportional with the dilution rate. The data from Table 1 shows clearly the benefits of a chromatographic system, where the valuable product compound is recovered with the higher concentrated raffinate. As the raffinate stream usually shows the higher concentration, whenever the elution order can be influenced, the method of choice should be the one where the desired product compound is being eluted with the raffinate stream.

As the process streams resulting from the SMB chromatography are higher concentrated, they enable a more efficient product recovery than those of the batch chromatography. With SMB, the required membrane area is smaller and the product loss is significantly lessened for both extract and raffinate treatment. This stresses the fact that for a comparison between SMB and batch chromatography, not only the productivity and efficiency of the separation have to be compared but also the product dilution and therefore the overall recovery costs.

Although, the calculated results coincide well with experimental data from literature, such data normally has to be acquired by previous laboratory or miniplant experiments for adaptation and verification of the model. Acquiring this data is usually a rather expensive and time-consuming procedure. Even if such data can be gathered from literature, it is not necessarily sufficiently exact or specific to allow thorough process simulation. For the comparison of batch and SMB chromatography and giving an insight into the advantages of process simulation, which did not require high quantitative accuracy of the simulated process parameters, the used literature data proved to be sufficient.

3.2. (B) Evaporation

The crystallization behavior and the induction time of the component system EN 21/ethylacetate/ethanol are only estimated from component data and the applied crystallization model. Therefore, a special evaporator type is employed to be able to cope with scaling by premature crystallization and to enable short residence times combined with high vaporization rates. The evaporator is modeled as a rotating film evaporator [19].

3.2.1. Model evaporation (rotating film evaporator)

The evaporator model was based on stepwise mass balancing along the heater surface (Fig. 6).

- Differential mass balance along the heater surface:

$$\dot{m}_{\mathrm{F}}(z+\mathrm{d}z)+\dot{m}_{\mathrm{D}}(z+\mathrm{d}z)=\dot{m}_{\mathrm{F}}(z)+\dot{m}_{\mathrm{D}}(z),$$

or $-\mathrm{d}m_{\mathrm{F}}(z)=\mathrm{d}m_{\mathrm{D}}(z)=\dot{m}''_{\mathrm{D}}(z)\,\mathrm{d}A_{\mathrm{H}}$.

- Mass balance for component i:

$$\dot{m}_{\mathrm{F}}(z)\,\mathrm{d}w_{i\mathrm{F}}(z)+\mathrm{d}\dot{m}_{\mathrm{F}}(z)w_{i\mathrm{F}}(z)=0.$$

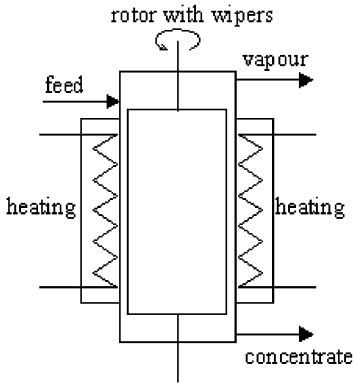

Fig. 6. Rotating film evaporator.

- Mass balance for solvent w:

$$\dot{m}_{\mathrm{F}}(z)\,\mathrm{d}w_{w\mathrm{F}}(z)+\mathrm{d}\dot{m}_{\mathrm{F}}(z)w_{w\mathrm{F}}(z)=-\mathrm{d}\dot{m}_{\mathrm{D}}(z)=-\dot{m}''_{\mathrm{D}}(z)\,\mathrm{d}A_{\mathrm{H}}.$$

- Energy balance:

$$Q_{\mathrm{H}}(z)=q_{\mathrm{H}}(z)\,\mathrm{d}A_{\mathrm{H}}=\dot{m}''_{\mathrm{D}}(z)\,\Delta h_{\mathrm{V}}\,\mathrm{d}A_{\mathrm{H}}+\dot{m}_{\mathrm{F}}(z)c_{\mathrm{PF}}(z)\,\Delta T_{\mathrm{bp}}(\mathrm{d}w_{i\mathrm{F}}),$$

with

$$q_{\mathrm{H}}(z)=k(T_{\mathrm{H}}-T_{\mathrm{F}}(z)).$$

- Increase in boiling point of the solvent w by the solute i:

$$\Delta T_{\mathrm{bp}}=\frac{RT_{\mathrm{bp},w}}{\Delta h_{\mathrm{V},w}M_{\mathrm{w}}}x_i.$$

- Heat transfer coefficient for the cylindrical heating surface:

$$k=\frac{1}{(1/\alpha_{\mathrm{b}})+(r_{\mathrm{b}}/\lambda_{\mathrm{W}})\ln(r_{\mathrm{a}}/r_{\mathrm{b}})\,(r_{\mathrm{b}}/r_{\mathrm{a}})(1/\alpha_{\mathrm{a}})}.$$

- The heat transfer coefficient α_{a} was estimated for condensing heating medium (e.g. steam) according to the water-film theory of Nusselt (Nusselt'sche Wasserhaut-Theorie).
- The heat transfer coefficient α_i for the evaporation area was calculated according to the empirical equations of Lutcha and Frank in [19] for this type of evaporator.

The evaporator is optimized according to the following criteria.

- A short residence time in the evaporator has to be achieved to undercut the induction time of the crystallization to reduce the risk of encrusting of the evaporation surfaces and to avoid a decrease in heat transfer rate.
- The supersaturation required by the crystallization step has to be provided. As at the same time, the remaining solution after crystallization is recycled into the evaporator, the dimensioning of the evaporator can only be done

in context with the crystallizer and the particle separator. The simulation results are given together for steps (B)–(D) in Section 3.5.

- The equipment and energy cost should be kept small as long as this does not impede with the more important criteria above. The equipment cost is proportional to equipment size, i.e. the heat transfer area, the energy cost is determined by the vaporization rate and the type of heating utility employed.

3.3. (C) Crystallization versus precipitation

The crystallization model is based on an ideal primary crystallization from a homogeneous solution. This relatively simple model allows adjusting crystallization rate by modification of the mean residence time in the crystallizer. The mean residence time determines the mean crystallite diameter, while the model determines the form of the particle size distribution.

The particle size distribution determines the yield of the crystallization, as only the fraction of the crystals above a limiting minimal diameter are recovered in the particle separator. The rest of the crystals remain in the solution and are recycled to the evaporator.

With increase in the recycle stream, its supersaturation decreases. The risk of encrusting also decreases with decreasing supersaturation of the recycled solution, which can be a quite desirable effect. A higher residence time in the crystallizer, i.e. a larger crystallizer, is then required to maintain a similar particle size distribution. Otherwise, the separation rate of the particle separator would diminish, as the crystal growth rate decreases with decreasing supersaturation and the particle size distribution shifts to smaller mean diameters.

The model equations of the crystallization are given in the following sections.

3.3.1. MSMPR crystallization model

According to Gnielinski et al. [20], Sattler [21], and Matz [22], this model assumes ideal mixing in a continuous batch reactor. The crystallization is described by nucleation rate, crystal growth rate, and the mass balance for steady state.

- Nucleation rate:

$$B = C_1 \exp\left[-\frac{C_2}{(\ln(c/c^*))^2}\right].$$

- Diffusion of the crystallizing compound from the bulk to the crystal surface:

$$m = k_D A(c - c_D).$$

- Integration of the molecules into the crystal grid (*n*th-order integration reaction):

$$m = k_R A(c_D - c^*)^n.$$

- Diameter distribution of the crystals:

$$n_i = n_{i0} \exp\left(-\frac{L}{G\tau}\right), \quad \text{with } \tau = \frac{\dot{V}}{V}.$$

- Total crystal surface A in the reactor:

$$A = \pi f_A V n_{i0} (\tau G)^3.$$

- Mass balance equations are as follows:
  - Crystallite yield $\dot{S}$:

$$\dot{S} = \frac{\dot{L}(w_1 - w_2) + \dot{D}_K w_2}{\mu - w_2(1-\mu)}.$$

  - Mass balance:

$$\dot{m} = \mu \dot{S},$$

$$\mu = \frac{\text{mass of dry crystals}}{\text{mass of wet crystals (including adhering solvent)}}.$$

- Nucleate density in the reactor n_{i0}:

$$n_{i0} = \frac{B}{G}.$$

3.3.2. Protein precipitation model

Protein precipitation model is based on the models in [23–25]. Assumed mechanism of precipitation is as follows:

1. injection of precipitation additives (salt, etc.);
2. nucleation;
3. diffusion-controlled growth (small aggregates);
4. flow-controlled growth (larger aggregates);
5. aggregation into flocks (flocculation);
6. particle separation (sedimentation, centrifugation, filtration).

3.3.2.1. Nucleation. Nucleation is almost instantaneous; negligible nucleation time.

3.3.2.2. Diffusion-controlled growth (perikinetic growth). Diffusion-controlled growth is also called perikinetic growth and is given as follows:

$$\frac{dc_P}{dt} = -\kappa c_P^2.$$

Rate constant:

$$\kappa = 8\pi D_{Pw} d_P N_A.$$

3.3.2.3. Flow-controlled growth (orthokinetic growth). There is minimal concentration of solved (molecular) protein. Further growth occurs by aggregation of smaller aggregates during particle collisions.

Starting time of flow-controlled growth after nucleation:

$$t_M = \frac{l^2}{4D_{iw}},$$

using the diameter of the turbulent eddies produced by stirring $l = \sqrt[4]{\rho\nu^3/(P/V)}$.

Growth kinetics of the *orthokinetic* growth:

$$-\frac{\mathrm{d}c_\mathrm{P}}{\mathrm{d}t} = \left(\frac{4}{\pi}\alpha\phi\sqrt{\frac{P/V}{\rho\nu}}\right)c_\mathrm{P},$$

with the constant volume fraction of precipitating protein in the reactor:

$$\phi = \tfrac{1}{6}(\pi d_\mathrm{P}^3)c_i N_\mathrm{A}.$$

3.4. (D) Particle recovery

The model of the particle separator is based on an ideal cut in the particle distribution at the limiting particle size (diameter). This assumes that all particles, i.e. crystallites, with a diameter larger or equal to the limiting diameter are recovered from the solution and can be fed to the drying stage.

As the crystallization model determines the particle size distribution, the particle separation model can be directly integrated into the crystallization model. This enhances simulation speed and efficiency, as interactions between these steps can be examined more easily.

The limiting particle size, the separation diameter of the particle separator, is the adjusting parameter of this step as it determines in combination with the particle size distribution the fraction of recovered solid product from the crystallization slurry and thus the efficiency of the whole crystallization.

The separation diameter was not adjusted to the changed particle size distributions, but kept constant at a chosen minimal product particle size. This should ensure a final solid product with constant handling properties and would also facilitate drying, as the time and effort required for stripping solvent rests from the solid product increases with decreasing particle size.

3.5. Optimization results for steps (B)–(D)

As after the pre-concentration stage, the streams should be identical for process engineering considerations, the differentiation between extract and raffinate resulting from batch or SMB chromatography is no longer relevant. The optimized parameter set for evaporation is given in Table 2.

The outlined evaporator could be acquired as a rotating film evaporator with an interior diameter (vaporization tube) of 30 cm (≅1 ft) and a tube height of 2.1 m (≅7 ft). The usual size range of rotating film evaporators is according to "Verfahrenstechnische Berechnungsmethoden" [19]: interior diameter: 8–90 cm; vaporization area: 0.125–16 m^2.

By increasing the recycle stream, the resulting mean residence time and the heater area can be reduced, as the heat transfer rate improves with increasing fluid velocities.

Table 2
Results of the process optimization for the evaporation step[a]

Feed (from pre-concentration)	
Rate (g/s)	7.5
Amount (mg/g)	14.4
Recycle (from crystallizer)	
Rate (g/s)	1.0
Amount (mg/g)	72.5
Total feed to evaporator	
Rate (g/s)	8.5
Amount (mg/g)	21.2
Concentrate	
Rate (g/s)	1.13
Amount (mg/g)	159
Vapor (g/s)	7.37
Evaporation area (m^2)	1.99
Residence time (s)	1.15
Vaporization heat (kW)	4.26
Pressure (=atmospheric) (bar)	1.0
Boiling temperature of inlet solution (°C)	77.1
Outlet temperature (°C)	79.0

[a] Rotating film evaporator; batch = SMB and extract = raffinate, i.e. differentiation between extract and raffinate resulting from batch or SMB chromatography is not relevant here.

As with increasing recycle volume, the concentration of the recycle can be reduced, the boiling point of the solution also decreases (Tables 3 and 4).

Applying a five times greater recycle stream for example would decrease the recycle concentration to 79.9 mg/g and reduce the required vaporization area by about 15% to 1.675 m^2. This would reduce the risk of encrusting of the product containing pipes and vessels, but would also require a five times larger crystallizer vessel to maintain the crystallization yield. Also the ability to control this evaporation with a mean evaporator residence time of about 0.5 s is questionable. With the increased vaporization rate, the amount of fluid carried out of the evaporator with the vapor stream

Table 3
Results for the process optimization of the crystallizer[a]

Crystallizer feed	
Rate (g/s)	1.13
Amount (mg/g)	21.2
Mean residence time (s)	832.7
Crystallizer volume (l)	1
Characteristic diameter of distribution (mm)	0.027
Rate of nucleation $(s\,m^3)^{-1}$	3.07×10^9
Radial rate of crystal growth (mm/s)	0.325×10^{-4}
Crystallite surface area (m^2)	5.865
Crystallization yield (wt.%)	111.6 (!)
Produced crystallite fraction	
Rate (g/s)	0.133
Amount (wt.%)	0.8

[a] Batch = SMB and extract = raffinate, i.e. differentiation between extract and raffinate resulting from batch or SMB chromatography is not relevant here.

Table 4
Results of process optimization for particle recovery[a]

Separation diameter (mm)	0.05
Recovered solid fraction (wt.%)	88.3
Resulting total process yield (%)	98.5 (=100% (!))
Recovered solid	
Rate (g/s)	0.133
Amount (wt.%)	0.8
Remaining solution (=recycle)	
Rate (g/s)	1.0
Amount (mg/g)	7.25

[a] Batch = SMB and extract = raffinate, i.e. differentiation between extract and raffinate resulting from batch or SMB chromatography is not relevant here.

as droplets would increase significantly as well. This would result in product loss and therefore to be avoided. Thus, the mean residence time is not reduced under 1 s.

Under the assumption that recycled crystallites (from the recycle stream) are totally resolved due to the higher temperature in the evaporator, the residence time of about 1 s should be adequate to undercut the induction time of crystallization.

As the costs for the crystallizer are negligible compared to those of the evaporator, the crystallizer is simply adjusted to the optimal dimensions of the evaporator.

The particle separator and thereby the separation diameter is selected for producing an adequately fine powder after drying of the recovered crystals. A higher mean residence time, i.e. a larger crystallizer, could achieve a better separation yield with the same separator by increasing the mean particle size of the crystals. But this would result in an increased recycle stream and thus a less optimal evaporation stage. Therefore, this measure was not taken.

Increasing the separation yield can become necessary, if the recycled crystallites would induce seeding in the recycle pipes and in the evaporator and would thus produce an intolerable amount of encrusting in these equipment parts.

The fraction of recycled crystals is equal to the difference of the crystallizer yield and the resulting total process yield of the evaporation/crystallization/particle recovery process unit. It is about 12 wt.% for these parameter conditions.

The yields are given as ratios to the total amount of crystallizable product in the feed stream, i.e. the product input of the process. So the crystallizer yield tends to be higher than 100 wt.%, because of the amount of recycled solid. The recycled fraction equals the percentage fraction above 100% for the balanced process.

This standardization illustrates the amount of product remaining in the process due to the recycle as a fraction of the product input.

3.6. (E) Drying and solvent recycle

As the drying and solvent recovery stages proved to be too complex to be satisfactorily modeled in the time frame of this study, they were not carried out. Especially the drying behavior proved to be too complex to create an efficient model or even procure a useful estimation of the drying process, especially without having relevant component and process data at hand.

To recycle, the solvent cannot be recommended for this task considering the required high purity of the product solution. As it would also increase the length and complexity of this study without necessity, it was not further researched. This was explained even by a cost calculation in detail in [11].

3.7. Error analysis

A decisive deviation is introduced into the simulation of the reverse osmosis and especially the evaporation stage by the increase in solution viscosity with the rising product concentration. As it was not reliable to estimate the viscosity increase on a purely theoretical basis, no such correction for the viscosity was introduced.

As vaporization rate is highly dependent on the flow velocity on the heater surface, the increase in viscosity could lead to aberrations of 5–10% from the calculated results. These aberrations would be transferred to all related parameters like residence time in the evaporator, required vaporization energy, and vaporization rate.

The aberration of the resulting total process yield after crystallization and particle recovery, which should result in 100% rather than 98.5%, is a result of a minor model weakness. The recovered crystal fraction still contains adhering solution, which is again still containing some dissolved product. The amount of this dissolved recovered product fraction could not be calculated exactly. This inaccuracy transfers also to the total process yield.

Also the deviation of the modeled crystallization from the real behavior could be considerable, because even the physical property data of the product was acquired by thermodynamic estimations based on the molecular structure of the compound. Thus important kinetic factors of crystallization had to be estimated on this basis with a considerable range of inaccuracy.

As the specific mechanisms of crystallization of the product are not known, many important effects could not be taken into account, like seeding effects by crystallites brought back into the crystallizer by the recycle.

Therefore, laboratory- and pilot plant-scale crystallization experiments are needed. For the mathematical modeling of seeding effects and resulting particle distributions in crystallization, there are many useful examples in literature (e.g. [26–29]). The applied simple MSMPR model should give a good impression of the crystallization behavior of a particular substance though.

The particle separator model deviates from a real separator by assuming ideal separation characteristics. For the MSMPR distribution from the crystallization model, the difference to a real separator cannot be greater than 1 or 2%,

as the separation diameter is adjusted to the lower end of the particle size distribution. Deviation from the MSMPR crystallization behavior would also make the particle separation results inaccurate, as the separation model is adjusted to the MSMPR distribution.

4. Conclusion

As outlined in the previous sections, process simulation is a powerful tool in process design and development, as shown for the product recovery and solvent recycling steps of chromatographic separation processes in the previous sections. In our example for the product recovery of the compound EMD 53986 (EN 21), it yielded detailed process data, which allowed already a great degree of complex process optimization. From the results for the refining strategy developed in the previous sections, several general conclusions can be drawn.

1. As chromatographic separation can be performed as SMB or batch processes, the refinement of the product solution was drawn up for both techniques and for raffinate and extract solutions. The SMB process requires in general less desorbent solvent, its product solutions are therefore more concentrated. As a consequence, the required membrane area for pre-concentration and thus the equipment cost is lower than that for the corresponding batch process. This difference can amount to 50% of the necessary membrane area for the SMB process. As the product loss increases with the amount of extracted solvent from the solution, the product loss for concentrating the more diluted product solution from the batch process to the same final concentration is about 15–50% higher than for the SMB process. These figures show clearly that for a fair comparison between different chromatographic methods, not only the productivity of the chromatographic step has to be taken into account but also the productivities and costs of the following steps in the production strategy. These steps can often show tremendous differences, so that the real economic advantage of an SMB separation over a batch separation may show up in the subsequent refining steps.
2. In precipitation and crystallization, the remaining solutions still contain a significant amount of product. They should be recycled to the concentrating stage and not be disposed off. Their direct disposal can increase the overall product loss to 50% of the product input. However, this must be considered against the risk of accumulation of impurities in the recycle.
3. Employing a membrane process for pre-concentration instead of evaporation can reduce the required amount of energy by more than 99%. Thus, membrane filtration should therefore be applied where technically feasible. The membrane process models allow a clearer insight into the estimation of the product loss than evaporation. Therefore, with membrane processes, the product loss can already be estimated in the simulation stage.
4. As SMB chromatography requires less solvent for product elution, its solvent recycling steps for solvent separation before disposal or solvent reuse in the chromatography would also be less cost intensive than for those for batch chromatography.

Finally, it has to be remarked that successful process design has to include and rely on laboratory- and pilot plant-scale experiments to detect and to quantify unaccounted and unaccountable effects and influences in the real processes. Only based on such experimental data, the reliability of the models can be checked and improved, as the models can be adjusted to the real process behavior. This would again greatly increase the efficiency of the process optimization by more exact computer simulations.

As most of the experiments can be conducted with relatively simple laboratory-scale equipment, it should be relatively easy and inexpensive to examine chromatographic separation processes in conjunction with the subsequent downstream refining processes to acquire an overall impression of their technical feasibility and economic efficiency.

References

[1] R. Gärtner, Prozessentwicklung und -optimierung der Produkt-Aufarbeitung und Lösungsmittel-Rückgewinnung nach chromatographischen Trennsequenzen durch die Unit Operations Kristallisation/Membrantechnik/Verdampfung, Graduate Thesis, University of Dortmund, 1998.
[2] R.K. Scopes, Protein Purification, Springer, Heidelberg, 1994.
[3] R.M. Devant, R. Jonas, M. Schulte, A. Keil, F. Charton, Enantiomer separation of a novel ca-sensitizing drug by simulated-moving-bed (SMB) chromatography, J. Prakt. Chem. 339 (1997) 315–321.
[4] M. Schulte, R. Ditz, R.M. Devant, J.N. Kinkel, F. Charton, Comparison of the specific productivity of different chiral stationary phases used for simulated moving bed chromatography, J. Chromatogr. 769 (1997) 93–100.
[5] R. Ditz, M. Schulte, J. Strube, Simulated moving bed chromatography technology in pharmaceutical new product development—first impact on the industry's race to the market, Curr. Opin. Drug Discovery Dev. 1 (3) (1998) 264–271.
[6] M. Schulte, Merck KGaA, 1997, unpublished results.
[7] VDI-Wärmeatlas, Berechnungsblätter für den Wärmeübergang, Vol. 6, VDI-Verlag, Düsseldorf, 1991.
[8] T.E. Daubert, R.P. Danner, Data Compilation Tables of Properties of Pure Compounds, Design Institute for Physical Property Data, American Institute of Chemical Engineers (AIChE), New York, 1987.
[9] J.A. Riddick, W.B. Bunger, T.K. Sakano, Organic Solvents—Physical Properties and Methods of Purification, Vol. 4, Wiley, New York, 1986.
[10] M. Mauz, R. Abbasi, K. Gerth, Kombination von Destillation und Pervaporation zur Rückgewinnung reiner Lösungsmittel aus Drogenextrakten, Pharm. Ind. 60 (3) (1998) 253–256.
[11] J. Strube, S. Haumreißer, H. Schmidt-Traub, M. Schulte, R. Ditz, Comparison of optimized batch and SMB chromatography, Org. Process Res. Dev. 1 (3) (1998) 264–271.
[12] R. Rautenbach, Membranverfahren—Grundlagen der Modul- und Anlagenauslegung, Springer, Berlin, 1997.
[13] H. Niemi, S. Palosaari, Flowsheet simulation of ultrafiltration and reverse osmosis processes, J. Membr. Sci. 91 (1994) 111–124.

[14] H. Niemi, S. Palosaari, Calculation of permeate flux and rejection in simulation of ultrafiltration and reverse osmosis processes, J. Membr. Sci. 84 (1993) 123–137.
[15] H. Mehdizadeh, J.M. Dickson, Modeling of reverse osmosis in the presence of strong solute membrane affinity, AIChE 39 (3) (1993) 434–445.
[16] R. Knauf, Umkehrosmose nicht-wäßriger Lösungen, Dissertation (Doctorate Thesis), RWTH Aachen, Shaker Verlag Aachen, 1996.
[17] R.J. Petersen, Composite reverse osmosis and nanofiltration membranes, J. Membr. Sci. 83 (1993) 81–150.
[18] R. Rautenbach, R. Albrecht, Membrantrennverfahren—Ultrafiltration und Umkehrosmose, Verlag Salle–Sauerländer, Fankfurt, 1981.
[19] Verfahrenstechnische Berechnungsmethoden -Teil 1: Wärmeübertrager, VCH, Weinheim, 1987.
[20] V. Gnielinski, A. Mersmann, F. Thurner, Verdampfung, Kristallisation, Trocknung, Vieweg, Braunschweig, 1993.
[21] K. Sattler, Thermische Trennverfahren—Grundlagen, Auslegung, Apparate, VCH, Weinheim, 1988.
[22] G. Matz, Kristallisation—Grundlagen und Technik, Springer, Berlin, 1969.
[23] P.A. Belter, E.L. Cussler, W.-S. Hu, Bioseparations—Downstream Processing for Biotechnology, Wiley, New York, 1988.
[24] J.E. Bailey, D.F. Ollis, Biochemical Engineering Fundamentals, 2nd Edition, McGraw-Hill, New York, 1986.
[25] C.E. Glatz, R.R. Fisher, Modeling of precipitation phenomena in protein recovery, in: J.A. Asenjo, J. Hong (Eds.), Separation, Recovery and Purification in Biotechnology—Recent Advances and Mathematical Modeling, ACS Symposium Series, American Chemical Society, Washington, DC, 1986.
[26] M.M. Clark, Transport Modelling for Environmental Engineers and Scientists, Wiley, New York, 1996.
[27] R.J. Farrel, Y.-Ch. Tsai, Modeling, simulation and kinetic parameter estimation in batch crystallization processes, AIChE 40 (4) (1994) 586–593.
[28] M. Bohlin, A.C. Rasmuson, Modeling of growth rate dispersion in batch cooling crystallization, AIChE 38 (12) (1992) 1853–1863.
[29] L.-D. Shiau, K.A. Berglund, Growth rate dispersion in batch crystallization, AIChE 36 (11) (1990) 1669–1679.